A P-type ATPase importer that discriminates between essential and toxic transition metals

Oded Lewinson[1], Allen T. Lee, and Douglas C. Rees[1]

Division of Chemistry and Chemical Engineering 114-96 and Howard Hughes Medical Institute, California Institute of Technology, Pasadena, CA 91125

Contributed by Douglas C. Rees, January 26, 2009 (sent for review October 15, 2008)

Transition metals, although being essential cofactors in many physiological processes, are toxic at elevated concentrations. Among the membrane-embedded transport proteins that maintain appropriate intracellular levels of transition metals are ATP-driven pumps belonging to the P-type ATPase superfamily. These metal transporters may be differentiated according to their substrate specificities, where the majority of pumps can extrude either silver and copper or zinc, cadmium, and lead. In the present report, we have established the substrate specificities of nine previously uncharacterized prokaryotic transition-metal P-type ATPases. We find that all of the newly identified exporters indeed fall into one of the two above-mentioned categories. In addition to these exporters, one importer, *Pseudomonas aeruginosa* Q9I147, was also identified. This protein, designated HmtA (heavy metal transporter A), exhibited a different substrate recognition profile from the exporters. In vivo metal susceptibility assays, intracellular metal measurements, and transport experiments all suggest that HmtA mediates the uptake of copper and zinc but not of silver, mercury, or cadmium. The substrate selectivity of this importer ensures the high-affinity uptake of essential metals, while avoiding intracellular contamination by their toxic counterparts.

membrane proteins | transition-metal homeostasis | heavy metal transporters | P_{1B} ATPases

Maintaining transition-metal homeostasis presents a unique challenge to all living organisms. Transition metals such as zinc, copper, and iron are essential to many physiological processes but are also toxic at elevated concentrations. Other metals, such as cadmium, silver, and mercury, exhibit acute toxicity by binding to macromolecules and perturbing their physiological interactions (1, 2). A diversity of membrane-embedded transporters translocate metals across the cell membrane, underlining the importance and the delicacy of this process. In prokaryotes, the concerted action of members of the RND, ABC, CDF, and P-type ATPase superfamilies functions to maintain appropriate intracellular concentrations of essential and toxic transition metals (3). In humans, perturbations in metal homeostasis lead to degenerative syndromes, cancer, and Wilson's and Menkes' diseases (4, 5).

P-type ATPases constitute a superfamily of transporters characterized by unique signature motifs. The hallmark of this family of pumps is the formation of a phosphoenzyme intermediate (hence the name P-type ATPase), by the transfer of the γ-phosphate from ATP to the highly conserved DKTGT motif (6). A family of P-type ATPases catalyzing the translocation of transition metals (also referred to as heavy-metal or type P_{1B} ATPases) has been identified (7, 8), with members present in all kingdoms of life. Such P-type ATPases harbor a Cys-Pro-Xaa (or Xaa-Pro-Cys) motif, with Xaa = Cys, Ser, or His, in their sixth transmembrane helix (TM6) that is essential for transport activity (7, 9, 10). Sequence homology of transition-metal P-type pumps further suggests a division into several subgroups with distinct substrate specificities. The majority of characterized pumps fall into one of the following categories: efflux pumps involved in detoxification of monovalent metals (copper[†] and silver) or efflux pumps involved in detoxification of divalent metals (zinc, cadmium, and mercury). These two groups differ in the presence of unique amino acid sequences in their transmembrane domains, presumably contributing to substrate specificity (7, 8). This notion is further supported by functional analysis of various P-type pumps harboring these amino acid motifs. In characterized systems (13, 14), pumps harboring amino acid sequences specific to monovalent metals indeed transported only copper and silver, whereas those harboring amino acid sequences specific to divalent metals transported only zinc, cadmium, and lead.

To further our understanding of substrate recognition by transition-metal pumps, we have cloned and expressed 18 uncharacterized prokaryotic P-type ATPases (15). Initially, we tested the abilities of the expressed proteins to restore tolerance to external concentrations of copper, silver, zinc, and cadmium in metal-sensitive *Escherichia coli* strains (16). By conducting dose–response experiments, we tentatively assigned the substrate specificity to 9 of the tested 18 genes. The 5 genes that unambiguously restored wild-type levels of metal tolerance segregated into two distinct groups; two genes restored tolerance toward zinc and cadmium but not to copper or silver, whereas the other three showed the reverse preference, as they conferred resistance only toward silver and copper. A sixth transporter, *Pseudomonas aeruginosa* Q9I147, could not be assigned to either subclass. In contrast to the pumps that restored metal tolerance to metal-sensitive strains, expression of this protein, which we have renamed HmtA (heavy metal transporter A), resulted in acute hypersensitivity with unique specificity. Hypersensitivity was observed only with metals that have clear functional roles and not with metals that are solely toxic. The results demonstrate a mechanism for a selective import by HmtA of the essential transition metals (copper and zinc), while avoiding detrimental intracellular accumulation of their toxic counterparts.

Results

In Vivo Characterization of Novel P-Type ATPases. We attempted to identify the substrate specificities of 18 uncharacterized prokaryotic P-type pumps (Table 1) by monitoring growth curves in the presence of increasing concentrations of copper, zinc, silver, and cadmium. All of the tested putative pumps contained the canonical P-type DKTGT (phosphorylation) motif. To avoid biasing the sampling, substrate-specific motifs were not used as a criterion for selection. The selected proteins were expressed in metal-sensitive *E. coli* strains (16), and their abilities to restore metal tolerance were evaluated in dose–response experiments. The optical density of the cultures was continuously monitored in an automated plate reader

Author contributions: O.L. and D.C.R. designed research; O.L. and A.T.L. performed research; O.L., A.T.L., and D.C.R. analyzed data; and O.L. and D.C.R. wrote the paper.

The authors declare no conflict of interest.

Freely available online through the PNAS open access option.

[1]To whom correspondence may be addressed. E-mail: lewinson@caltech.edu or dcrees@caltech.edu.

[†]Assignment of the appropriate oxidation state of copper in in vivo studies is challenging due to the presence of two physiologically relevant species, Cu^{+} and Cu^{2+}. In these studies, copper is supplied in the Cu^{2+} form, and will remain in this state under the aerobic growth conditions. Because the cytoplasm provides a reducing environment (11, 12), the intracellular form should be predominantly Cu^{+}. With these reference states, copper importers in this study are assumed to be specific for Cu^{2+}, whereas copper exporters are assumed to be specific for Cu^{+}.

Table 1. List of strains and P-type ATPases used in this work

Source organism of protein	Accession no.	Minimal inhibitory concentration*				Classification
		Cu^{2+}, mM	Ag^{+}, μM	Zn^{2+}, mM	Cd^{2+}, μM	
E. coli W3110 (insensitive to metals)		4.2	22	2	1,200	
E. coli GG44 (sensitive to Cu^{2+}, Ag^{+})		1.2	7	1.8	1,050	
E. coli GG48 (sensitive to Zn^{2+}, Cd^{2+})		3.9	19	0.16	3.1	
Campylobacter jejuni	Q0P9A1	0.9	3.11	0.12	6.6	Unassigned
C. jejuni	Q0P995	0.5	1.1	0.11	2.1	Unassigned
C. jejuni	Q0PAK1	1.2	3	0.16	3.2	Unassigned
Pyrococcus furiosus	Q8TH11	3.9	13.2	0.14	12	Cu^{+}/Ag^{+} exporter
Helicobacter pylori	O26033	1.3	2.2	0.18	2.7	Unassigned
Rhizobium radiobacter	Q7D0J8	1.9	2.5	2.1	1,100	Zn^{2+}/Cd^{2+} exporter
R. radiobacter	A9CJE3	4.4	15.2	0.13	4.1	Cu^{+}/Ag^{+} exporter
R. radiobacter	A9CJP7	4.1	17.4	0.12	4.4	Cu^{+}/Ag^{+} exporter
R. radiobacter	A9CIZ1	1.8	5.3	0.16	3.6	Putative Cu^{+}/Ag^{+} exporter
Streptococcus pneumoniae	Q97RR4	1.3	2.7	0.14	5.2	Unassigned
S. pneumoniae	Q97NE2	1.1	2.3	0.19	4.8	Unassigned
S. pneumoniae	Q97PQ2	1	3.4	0.19	4.8	Unassigned
S. pneumoniae	P35597	0.8	3.3	0.42	27	Putative Zn^{2+}/Cd^{2+} exporter
Pseudomonas aeruginosa	Q9HXV0	1.3	3.6	1.8	800	Zn^{2+}/Cd^{2+} exporter
P. aeruginosa	Q9HX93	0.8	2.7	0.11	2.2	Unassigned
P. aeruginosa	Q9I147	0.04	3.1	0.035	3.2	Cu^{2+}/Zn^{2+} importer
P. aeruginosa	Q9I3G8	1.55	5.2	0.15	9.5	Putative Cu^{+}/Ag^{+} exporter
P. aeruginosa	Q9HUY5	0.8	4.1	0.9	5.7	Unassigned

*Values presented are minimum inhibitory concentrations in millimolar or micromolar (as indicated) when the tested gene was expressed in the appropriate metal-sensitive mutant strain. The wild-type W3110 strain, insensitive to metals, was transformed with an empty plasmid.

over a broad range of metal concentrations so that minimal inhibitory concentrations (MICs) could be determined. A zinc toxicity assay is shown in Fig. 1*A*, demonstrating the growth phenotypes of active and inactive test proteins. Fig. 1*B* shows how the MICs were calculated from an ensemble of similar assays of copper toxicity, and Table 1 summarizes the results obtained for all tested proteins. Of the 18 surveyed proteins, 4 (Q0PAK1, Q97NE2, Q97PQ2, and Q9HUY5) lacked the CPX sequence motif associated with the family of transition-metal P-type ATPases, and indeed, no metal-related phenotype was observed for any of these pumps. Unambiguous assignment of substrate specificity could be established for 6 of the tested proteins (Q8TH11, Q7D0J8, A9CJE3, A9CJP7, Q9HXV0, and Q9I147), all of which contained the CPX motif. Putative functions were assigned to 3 additional pumps (A9CIZ1, P35597, and Q9I3G8). Because of low levels of activity, however, these latter assignments are tentative (Table 1). Five of 6 pumps that were unambiguously characterized (Q8TH11, Q7D0J8, A9CJE3, A9CJP7, and Q9HXV0) restored wild-type levels of metal tolerance. These 5 pumps exhibit the properties expected of metal exporters and could be segregated into two distinct groups: 2 pumps that conferred resistance to zinc and cadmium (Q7D0J8 and Q9HXV0) and 3 pumps that conferred resistance to copper and silver (Q8TH11, A9CJE3, and A9CJP7). Each of these substrate-specific subsets contained distinct conserved sequences in predicted transmembrane domains, presumably defining substrate specificity (see *Discussion* for detailed analysis).

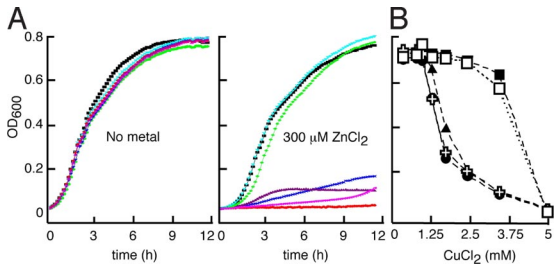

Fig. 1. Metal sensitivity assays. (*A*) *Escherichia coli* wild-type cells (black traces) or *E. coli* metal-sensitive strain (all other traces) were cultured in the absence (*Left*) or presence (*Right*) of 300 μM $ZnCl_2$. Optical density at 600 nm was continuously monitored. Cells were transformed with an empty, control plasmid (purple and black traces) or with a plasmid encoding *R. radiobacter* Q7D0J8 (green), *Pseudomonas aeruginosa* Q9HXVO (cyan), *S. pneumoniae* Q97PQ2 (blue), *P. aeruginosa* Q9HUY5 (red), or *P. aeruginosa* Q9HX93 (magenta). (*B*) Optical density of cells after 12-h growth in the presence of the indicated $CuCl_2$ concentrations. *E. coli* wild-type cells insensitive to metals (filled squares) or *E. coli* metal-sensitive strain (all other traces) were transformed with an empty plasmid (circles), plasmid encoding *R. radiobacter* A9CJE3 (open squares), *P. aeruginosa* Q913G8 (triangles), or *P. aeruginosa* Q9HXVO (crosses). Such plots were used to calculate minimal inhibitory concentrations and generate the data in Table 1.

HmtA Confers Selective Hypersensitivity to Metals. Remarkably, expression of one of the tested proteins, *P. aeruginosa* Q9I147 (HmtA), resulted in acute hypersensitivity toward copper. Growth of cells expressing this protein was inhibited at copper concentrations as low as 12 μM. Under identical conditions and even in the presence of 0.7 mM $CuCl_2$, control cells showed very little growth inhibition (Figs. 2 and 3*A*). The time course of the copper-induced growth inhibition directly correlated with that of HmtA expression. In the first 2 h of growth, no copper sensitivity was observed, and also no expression of HmtA was detected by Western blot analysis. Growth inhibition was observed only when membrane-associated HmtA expression could be detected (Fig. 2 *Inset*). Several control experiments (Fig. 3) were conducted to test the relevance of this ≈60-fold increase in copper susceptibility. In the absence of copper,

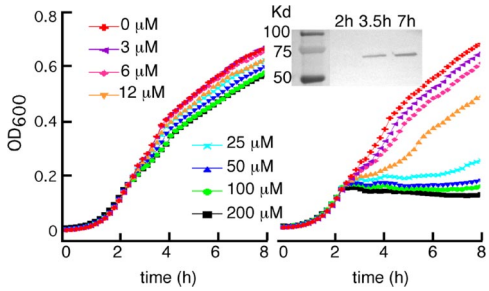

Fig. 2. HmtA-associated copper hypersensitivity. *E. coli* metal-sensitive cells were transformed with a control plasmid (*Left*) or HmtA-encoding plasmid (*Right*). Growth in the presence of the indicated $CuCl_2$ concentrations was continuously monitored. (*Inset*) Time-dependent HmtA expression by immunoblot detection.

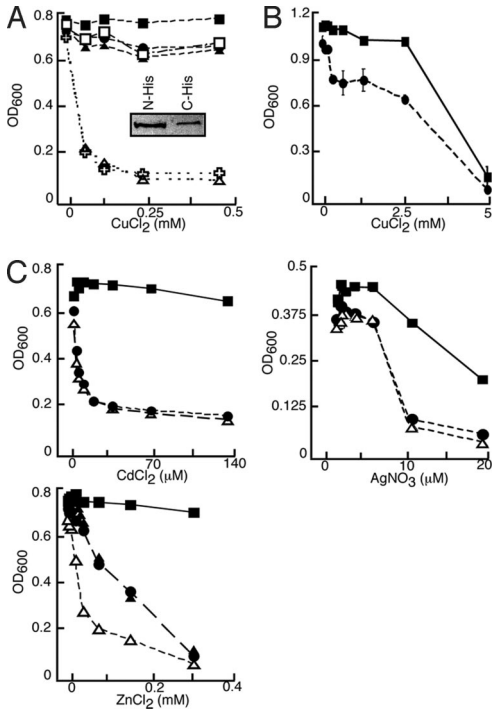

Fig. 3. Metal selectivity of HmtA. (*A*) The optical density at 600 nm of *Escherichia coli* cells cultured for 12 h in the presence of the indicated concentrations of $CuCl_2$. The filled squares represent *E. coli* wild-type cells transformed with an empty plasmid. All other traces depict an *E. coli* metal-sensitive strain transformed with different plasmids: an empty plasmid (filled circles), native HmtA in the absence of the inducer L-arabinose (open squares), an N-terminal His-tagged version of HmtA (full triangles), a C-terminal His-tagged version of HmtA (crosses), and native HmtA (open triangles). (*Inset*) SDS/PAGE immunoblot detection of the relative amounts of C-His HmtA and N-His HmtA in the membrane fraction. (*B*) $CuCl_2$ sensitivity in *Pseudomonas aeruginosa*. The optical density at 600 nm of wild-type *P. aeruginosa* (filled circles) or a mutant strain deleted of HmtA (filled squares) grown for 12 h in the presence of the indicated $CuCl_2$ concentrations is shown. (*C*) $CdCl_2$, $AgNO_3$, and $ZnCl_2$ sensitivity in *E. coli*. The optical density at 600 nm of *E. coli* cells cultured for 12 h in the presence of the indicated metal concentrations is shown. The filled squares represent *E. coli* wild-type cells transformed with an empty plasmid. The other traces depict an *E. coli* metal-sensitive strain transformed with either an empty plasmid (filled circles) or a C-terminal His-tagged version of HmtA (open triangles). The growth of the latter cells in the absence of the inducer L-arabinose is shown only for $ZnCl_2$ sensitivity (filled triangles).

induction of protein expression did not result in toxicity. Similarly, in the presence of copper but in the absence of the inducer for protein expression (L-arabinose) no toxic effect was observed (Fig. 3*A*).

We have previously observed that the function of heavy-metal P-type pumps greatly depends on the location of the fused affinity tag (15). Our initial observation of the toxic effect conferred by HmtA was using a native, untagged version of the protein. We generated two other constructs, His-tagged at either the N terminus or the C terminus. Despite being expressed at higher levels in the membrane (Fig. 3*A Inset*), the N-terminally tagged protein did not render cells susceptible to copper. Expression of the C-terminally tagged protein resulted in increased copper sensitivity, virtually identical to the sensitivity induced by the native form. To account for effects of the heterologous expression, we examined the growth profile of a *P. aeruginosa* strain where the gene encoding HmtA was disrupted (17). We compared the growth of this strain (PA2435-421) to the growth of the parental wild-type strain. Fig. 3*B* shows that under conditions of high extracellular copper (>300 μM) the deletion strain has a small yet significant growth advantage over the parental strain. Thus, in both *E. coli* and *P. aeruginosa* cells, expression of HmtA results in increased copper sensitivity.

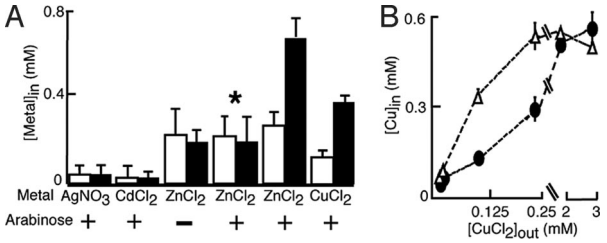

Fig. 4. Expression of HmtA results in increased intracellular metal concentrations. (*A*) *E. coli* metal-sensitive strains transformed with control plasmid (open bars) or HmtA-encoding plasmid (full bars) were cultured in the presence of 2.5 μM $AgNO_3$, 2.5 μM $CdCl_2$, 75 μM $CuCl_2$, or 75 μM $ZnCl_2$. Cells were harvested and washed with metal-free buffer, and total internal metal concentrations were measured by inductively coupled plasma mass spectroscopy. The asterisk denotes cells that were harvested early in the growth, before initiation of HmtA expression. Error bars represent standard deviations of three repeats. (*B*) Internal copper concentrations as a function of external copper in control cells (circles) or HmtA-expressing cells (triangles). Bars represent standard deviations of three repeats.

We next examined whether the increased susceptibility was limited to copper or was also extended to other transition metals. Fig. 3*C* and Table 1 show that tolerance toward either cadmium or silver was unaffected by expression of HmtA. However, zinc toxicity significantly increased when expression was induced. Similar to what has been observed with copper, zinc susceptibility was observed only when expression of HmtA was induced (i.e., in the presence of L-arabinose) and was not observed when the nonfunctional N-terminally tagged protein was expressed (Fig. 3*C*).

Expression of HmtA Leads to Increased Intracellular Concentrations of Copper and Zinc but Not of Silver or Cadmium. A possible explanation for the increased sensitivity toward zinc and copper is that higher levels of these metals are accumulated in the susceptible cells. This would imply that HmtA functions as a metal importer specific for these metals. To test this hypothesis, total internal metal contents of control and HmtA-expressing cells were measured by inductively coupled plasma mass spectroscopy (ICP-MS) (see *Materials and Methods* for details). Total internal volume was estimated by counting colonies of serial dilutions of cultures and assuming a volume of 10^{-15} L per cell (18). Similar to what was observed in the growth assays, when L-arabinose was omitted from the growth medium, no difference in intracellular metal concentrations was detected between control and HmtA-expressing cells (Fig. 4*A*). When cells were cultured in the presence of either $CdCl_2$ or $AgNO_3$, similar amounts of these metals were accumulated regardless of HmtA expression. In contrast, when either $CuCl_2$ or $ZnCl_2$ was included in the growth medium, significantly higher levels of these metals were associated with expression of HmtA (Fig. 4). When cells were harvested early during the growth, before HmtA could be expressed (Fig. 2 *Inset*), no increase in metal content was measured. Although a 2- to 3-fold increase in the total intracellular metal concentration may seem modest, relative to the background of essentially no free intracellular copper or zinc under normal cellular conditions (19), such an increase could correspond to a significant increase in the concentration of free intracellular metal, thus accounting for the observed toxicity.

Cells Expressing HmtA Accumulate Critical Intracellular Levels of Copper at Low External Copper Concentrations. When control or HmtA-expressing cells are cultured in the presence of very low (<5 μM) or very high (>1 mM) $CuCl_2$ concentrations, no significant differences in growth rates are observed (Fig. 2). Only at intermediate concentrations (10–250 μM) are significant differences in growth rates observed. Fig. 4*B* shows the total internal copper concentrations of cells cultured in $CuCl_2$ concentrations from1 μM to 3 mM. At low external $CuCl_2$ concentrations, similar intracellular

BIOCHEMISTRY

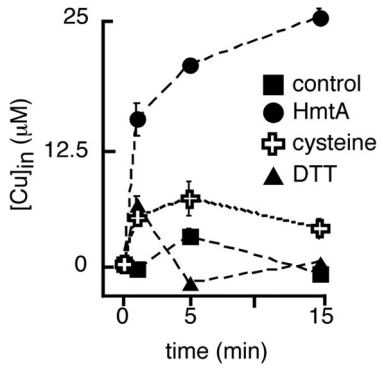

Fig. 5. Time-dependent copper uptake. Cells transformed with empty plasmid (squares) or HmtA-encoding plasmid (all other traces) were cultured in the absence of metals, washed with metal-free buffer, and allowed to recover in the presence of glucose. Transport was initiated by the addition of 250 nM $CuCl_2$, and samples were withdrawn at the indicated times. Where indicated, 0.5 mM DTT or 0.25 mM cysteine was included in the reaction mixture. Total internal metal concentrations were measured by inductively coupled plasma mass spectroscopy. Error bars represent standard deviations of three repeats.

metal contents were measured in control and HmtA-expressing cells. Such was also the case at the high end of the concentration scale. However, at intermediate concentrations, up to 3.5-fold more total copper was found in cells expressing HmtA. At ≈75 μM external $CuCl_2$, HmtA-expressing cells accumulate roughly 0.3 mM $CuCl_2$.

This is also the concentration where these cells undergo almost complete growth arrest, whereas control cells are hardly affected. A much higher external $CuCl_2$ concentration (>1 mM) is needed to raise the intracellular copper content of control cells to such levels. Importantly, for both cell types, significant (50–80%) growth arrest is observed only when internal copper is >0.3 mM. It thus seems that expression of HmtA does not alter the threshold for cell death but rather alters the external metal concentration at which this threshold is crossed.

HmtA-mediated metal transport was further investigated by performing time-dependent uptake experiments. Control or HmtA-expressing cells were grown in standard Luria Bertani (LB) medium, without the addition of any metals. Cells were then harvested and washed with a metal-free buffer. After recovery at 35 °C in the presence of glucose, $CuCl_2$ was added to initiate transport. At the indicated time points (Fig. 5), samples were withdrawn, and the intracellular metal concentrations were measured by ICP-MS. When $CuCl_2$ was added at concentrations of 25–250 nM, little or no metal uptake was detected in control cells. This observation suggests that under the experimental conditions *E. coli* cells lack an uptake system of sufficiently high affinity. In contrast, cells expressing HmtA take up copper on a time scale that nears saturation within 4–5 min. When $CuCl_2$ was added at 250 nM, the total internal concentration reached ≈25 μM within 15 min (Fig. 5). The 50- to 100-fold increase in copper uptake observed in HmtA-expressing cells (relative to control cells) at submicromolar concentrations is suggestive of a high-affinity uptake system.

For Cu^+/Ag^+ and for Zn^{2+}/Cd^{2+} P-type exporters, concomitant addition of cysteine with metals has been shown to stimulate activity, suggesting that the actual substrate of heavy-metal exporters is not the hydrated metal ion but rather a thiol-complexed species (13, 20, 21). We tested whether the stimulatory effect of cysteines observed with metal exporters also holds true for a metal importer. Addition of 0.25 mM cysteine to a reaction mixture containing 250 nM $CuCl_2$ did not stimulate activity but rather resulted in reduced copper transport by HmtA. Diminished copper uptake was also observed when 0.5 mM DTT was added together with $CuCl_2$ (Fig. 5). Similar inhibition by DTT (and other reducing agents) has been reported for cupric (Cu^{2+}) exporters, whereas a stimulatory effect of DTT has been observed with cuprous (Cu^+) exporters (13, 22).

Discussion

Substrate Specificity of Transition-Metal P-Type ATPases. Due to the chemical similarities between Cu^+ and Ag^+ and between Zn^{2+} and Cd^{2+}, it is not surprising that P-type exporters specialize in detoxifying one of these two subsets (7, 13, 14, 21, 23, 24). We have determined the metal specificities for 5 previously uncharacterized P-type transition-metal exporters, along with tentative assignments for 3 additional pumps exhibiting low levels of activity. Regardless of the level of activity, each of these 8 pumps may be assigned to one of the two anticipated substrate-specific categories (Table 1). For a metal importer, however, such a substrate recognition profile would clearly be detrimental. For example, although copper is an essential element, Ag^+ has been broadly used as a bactericide. Similar considerations disfavor recognition of both Zn^{2+} (essential) and Cd^{2+} (toxic) by the same importer. Initial indications that HmtA only mediates the transport of the essential transition metals were provided by in vivo metal tolerance assays (Figs. 2 and 3). The hypersensitivity observed in these assays was shown to correlate with elevated levels of intracellular metals (Fig. 4). The severity of the toxic effects, especially with copper, demonstrates the consequences of disruption of heavy-metal homeostasis, achieved here by the introduction of a foreign, unregulated transporter. Deletion of the chromosomal copy of the gene encoding HmtA resulted in a *P. aeruginosa* strain that was mildly more resistant to copper and zinc, again suggesting involvement of the gene in metal uptake. A similar increase in copper resistance was observed upon deletion of CtaA, a copper importer of *Synechococcus* (25). Robust metal uptake by HmtA could be detected at the nanomolar range, and a 50- to 100-fold gradient in total intracellular copper was generated within 10–15 min. Transport was inhibited by thiols, suggesting that the transported moiety is the uncomplexed metal ion (Fig. 5). The inhibition by cysteine sets HmtA apart from the corresponding exporters, because in all tested cases cysteine was found to be stimulatory.

Putative Amino Acid Motifs Contributing to Substrate Specificity. Sequence comparisons (6) and functional characterization (26, 27) of P-type ATPases have underlined the importance of the CPX motif in TM6 for heavy-metal transport. We have tested the importance of this motif by comparing the in vivo activities of P-type ATPases that harbor or lack this motif. No activity could be detected with any of the tested metals for proteins lacking this motif. In contrast, all of the proteins that conferred any metal tolerance contained some variation of this motif (Table 1). These findings lend strong support to the notion that the CPX motif located in TM6 has a central role in heavy-metal transport.

To identify amino acid motifs that may contribute to substrate specificity, we aligned the amino acid sequences of the 6 newly characterized transporters to the sequences of 6 metal pumps of known substrate specificities (Fig. 6). Due to the small number of aligned sequences, we looked for regions of conservation rather than specific conserved positions. Of particular interest were amino acid motifs that were conserved within each subgroup yet differed between them. In all of the aligned sequences, full conservation was observed for the general P-type signature motifs that are involved in ATP binding and hydrolysis and are not specific to transition-metal transport (6). Very little sequence conservation was observed in TM helices 1–3, regardless of substrate specificity. In contrast, TM helices 4–8 showed high degrees of conservation, with substantial substrate-specific divergence (Fig. 6). Both substrate-specific subgroups harbor the canonical CPX motif in TM6. However, in Zn^{2+}/Cd^{2+} pumps, this motif is preceded by an additional WIYR/K motif, which is absent in Cu^+/Ag^+ pumps. TM6 of Zn^{2+}/Cd^{2+} pumps is also more polar than that of Cu^+/Ag^+ pumps, containing additional Ser, Tyr, and Arg or Lys residues. Several conserved positions harbor residues of very different properties in

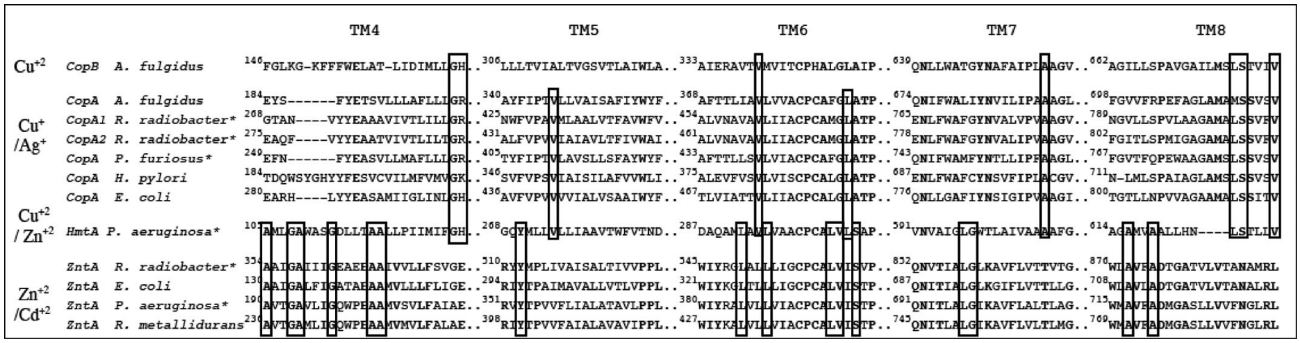

Fig. 6. Amino acid sequence alignment of transmembrane domains 4–8 of Cu^{+}/Ag^{+}, Cu^{2+}, Zn^{2+}/Cd^{2+}, or Cu^{2+}/Zn^{2+} P-type ATPase pumps. Conserved amino acids are in bold, and numbers in superscript represent amino acid positions. Proteins identified in this work are denoted by an asterisk. Boxes highlight positions where HmtA residues are conserved with residues of either Cu^{+}/Ag^{+} pumps or Zn^{2+}/Cd^{2+} pumps.

each of the subgroups. One example is Asn of TM7 of Cu^{+}/Ag^{+} pumps, which is paralleled by Lys in Zn^{2+}/Cd^{2+} pumps. Another is Asp of TM8 of Zn^{2+}/Cd^{2+} pumps, which is paralleled by Pro in Cu^{+}/Ag^{+} exporters. Importantly, mutational analyses of these residues (23, 28) have demonstrated their importance for metal recognition. The newly identified WIYR/K motif (TM6) and Lys of TM7 (both specific to Zn^{2+}/Cd^{2+} pumps) present attractive targets for future studies.

The predictive value of these alignments can perhaps be appreciated by examining the sequence of CopB of *Archaeoglobus fulgidus* (22). This Cu^{2+} exporter aligns well with Cu^{+}/Ag^{+} pump exporters, albeit with several subtle substitutions of conserved residues in TMs 5, 6, and 8 (Fig. 6). It is attractive to hypothesize that these differences may contribute to the discrimination between Cu^{2+} and Cu^{+}. These findings support and expand upon a previous classification of the sequence determinants underlying the substrate specificities of heavy-metal-transporting P-type ATPases (7, 8). The amino acid sequence of HmtA, the only transition-metal importer identified in this work, readily aligns with the sequences of both Zn^{2+}/Cd^{2+} and Cu^{+}/Ag^{+} exporters (Fig. 6). Interestingly, HmtA shows alternating substrate-specific conservation with both subgroups. For example, the N terminus of TM4 of HmtA harbors 6 of the 8 conserved residues of Zn^{2+}/Cd^{2+} exporters. In contrast, the C terminus harbors the conserved His/Lys/Arg of Cu^{+}/Ag^{+} exporters (corresponding to Glu in Zn^{2+}/Cd^{2+} exporters). The CPC motif of TM6 of HmtA is followed by the conserved Ser of Zn^{2+}/Cd^{2+} exporters, whereas TM8 lacks the conserved Asp residue that has been shown to be functionally essential to this subgroup (28). The lack of conservation of this catalytically crucial Asp is highlighted by the conservation of a Ser residue that has been shown to participate in Cu^{+}/Ag^{+} recognition (23).

In addition to the above-mentioned substrate-dependent sequence divergence, global topological and hydrophobicity analyses suggest that the difference between pumps of different substrate specificity may not be restricted to the identified motifs in TMs 4, 5, 6, 7, and 8. Fig. 7 shows the topology predictions for 6 Cu^{+}/Ag^{+} or Zn^{2+}/Cd^{2+} pumps. Regardless of the accuracy of these predictions, the clustering of these pumps into distinct topological profiles according to their substrate specificity suggests that structural distinctions exist beyond local variations in sequence. It is tempting to hypothesize that such "topological clustering" may be used as a predictive tool for substrate specificity of heavy-metal-transporting P-type pumps. In this regard, it is interesting to note that Mg^{2+} transporters fall into yet a third, distinct subgroup (Fig. 7). The topological profile of HmtA (Fig. 7) resembles more the profile of Zn^{2+}/Cd^{2+} pumps than that of Cu^{+}/Ag^{+} pumps. This perhaps reflects the fact that the majority of the conserved residues in HmtA (14 out of 21) are derived from the signature motifs of Zn^{2+}/Cd^{2+} pumps.

Homologues of HmtA. To date, no high-affinity copper uptake system has been identified in laboratory strains of *E. coli*. Indeed, control cells, which are W3110 derivatives, showed very little uptake of copper in the nanomolar range (Fig. 5). A BLAST search of *E. coli* strains finds, in addition to the CopA and ZntA exporters, 3 HmtA homologues from nonlaboratory *E. coli* strains. It is attractive to hypothesize that one of these proteins is the missing metal importer. These 3 homologues were identified in circumstances that have some relation to pathogenicity and virulence: SilP was identified in a avian pathogenic *E. coli* strain, whereas HRA-1 and HRA-2 were identified as contaminants of a cDNA library prepared from human intestine (29, 30). Intriguingly, although degenerate primers were used in the latter work, the *E. coli copA* and *zntA* genes were not amplified. Possibly, under infectious conditions, higher transcript levels of HRA-1 and HRA-2 resulted in their amplification and inclusion in the cDNA library. A direct role in virulence has been indicated for an HmtA homologue, the *Listeria monocytogenes* heavy-metal P-type pump CtpA. Chromosomal deletion of *ctpA* resulted in an *L. monocytogenes* strain with

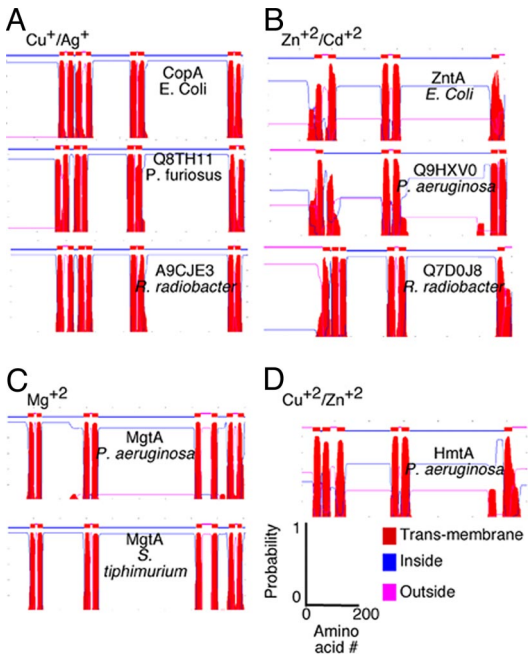

Fig. 7. Topological predictions using TMHMM (35) for Cu^{+}/Ag^{+} (*A*), Zn^{2+}/Cd^{2+} (*B*), Mg^{2+} (*C*), or Cu^{2+}/Zn^{2+} (*D*) P-type pumps. Red bars indicate transmembrane domains, blue lines indicate intracellular loops, and magenta lines indicate extracellular loops.

dramatically impaired infectivity (31). A role for heavy-metal-transporting P-type ATPases in virulence is perhaps not so surprising in light of the emerging role of metal homeostasis in host–pathogen interactions (32, 33).

In conclusion, the results presented here suggest that transition-metal P-type exporters and importers differ with respect to their substrate recognition profiles. Although the exporters extrude both the essential and the nonessential transition metals, an importer will bring in only biologically essential metals. The high affinity and selectivity of the importer provide a simple yet effective mechanism for the acquisition of essential transition metals while avoiding cross-contamination with their toxic counterparts.

Materials and Methods

Metal Sensitivity Assays. *E. coli* strains GG44 or GG48 (16) were used for Cu^{+}/Ag^{+} or Zn^{2+}/Cd^{2+} sensitivity assays, respectively. In all assays, *E. coli* W3110 (insensitive to metals) was included as a positive control. For $CuCl_2$, $ZnCl_2$, and $CdCl_2$ toxicity assays, overnight cultures (in LB medium supplemented with 30 μg/mL kanamycin and 100 μL/mL carbenicillin) were diluted to an optical density (600 nm) of 0.05 in 150 μL of the same medium in the absence or presence of 0.05% L-arabinose. Growth of cells was continuously monitored (in dark conditions) in an automated plate reader (Saffire II; Tecan). $AgNO_3$ toxicity assays were similarly performed using a modified M9 minimal medium (no added chloride), in which calcium and ammonium are added as acetate salts and glycerol serves as the carbon source. Metals were freshly prepared as solutions of $CuCl_2$, $ZnCl_2$, $AgNO_3$, and $CdCl_2$. Minimal inhibitory concentrations were calculated as the concentration needed to inhibit growth by 50% relative to growth in the absence of metals.

Sequence Alignment and Topology Analysis. Multiple sequence alignment of *A. fulgidus* CopA (23), *R. radiobacter* CopA1, *R. radiobacter* CopA2, *P. furiosus* CopA, *R. radiobacter* ZntA, *P. aeruginosa* ZntA (this work), *Helicobacter pylori* CopA (34), *E. coli* CopA (13), *A. fulgidus* CopB (22), *E. coli* ZntA (14), and *Ralstonia metallidurans* ZntA (24) was performed with the program CLUSTALW (www.ebi.ac.uk/Tools/clustalw2). Topology predictions were generated using the TMHMM server, using default settings (www.cbs.dtu.dk/services/TMHMM-2.0) (35).

Membrane-Associated Expression of HmtA. Cultures of GG44/pBad HmtA-6HIS or GG44/pBad 6HIS-HmtA were grown in LB medium supplemented with 30 μg/mL kanamycin, 100 μL/mL carbenicillin, and 0.05% L-arabinose. Cells were harvested at the indicated times and placed on ice for 30 min. After disruption by sonication, debris was removed by centrifugation at 10,000 $\times$ *g* for 10 min, and membranes were collected by ultracentrifugation at 150,000 $\times$ *g* for 30 min. His-tagged protein content of the membrane fraction was analyzed by immunoblot SDS/PAGE.

Measurements of Internal Metal Concentrations. *E. coli* strains GG44 or GG48 were used for Cu^{+}/Ag^{+} or Zn^{2+}/Cd^{2+} accumulation assays, respectively. Cultures were diluted to an optical density (600 nm) of 0.05 in LB medium supplemented with 30 μg/mL kanamycin, 100 μL/mL carbenicillin, 0.05% L-arabinose, and the indicated metal concentration. Cells were grown for 7–8 h and placed on ice for 30 min. Equivalent amounts of cells [2 mL of cells at an optical density (600 nm) of 0.4] were harvested by spinning for 10 s at 15,000 $\times$ *g* and washed with 1 mL of ice-cold 50 mM Tris·HCl (pH 7.5), 100 mM KCl. (All solutions were prepared with HPLC-grade water.) Cells were resuspended in 2.5 mL of HPLC-grade water, and metal contents were directly measured by using a Hewlett-Packard 4500 Inductively Coupled Plasma Mass Spectrometry system (Environmental Analysis Center, California Institute of Technology). The metal content of cells grown in the absence of metal to which the appropriate metal concentration was added just before the wash step (representing nonspecific metal binding) was subtracted from each sample. To estimate total internal volume of cells, cultures were plated as a series of 3-fold dilutions on LB-agar plates. Three such dilutions were counted and averaged, and total internal volume was estimated by multiplying the number of cells by 10^{-15} L [the volume of a single cell (18)].

Transport Assay. Cultures were grown (in the absence of metals) to an optical density (600 nm) of 1.3–1.5 in LB medium supplemented with 30 μg/mL kanamycin, 100 μL/mL carbenicillin, and 0.05% L-arabinose. Before harvest, cells were placed on ice for 30 min. Cells were washed with 50 mM potassium phosphate (pH 7.5), 2 mM $MgCl_2$ (made with HPLC-grade water) and resuspended with the same buffer to an optical density of 2.5. After 10 min of recovery in the presence of 0.2% glucose (35 °C, shaking at 250 rpm), transport was initiated by addition of the desired metal concentration. At the indicated time points, a 0.5-mL sample was withdrawn, pelleted, and washed with 50 mM potassium phosphate (pH 7.5). Cells were resuspended in 2.5 mL of HPLC-grade water, and metal contents were directly measured by using ICP-MS. Nonspecific metal uptake was subtracted from each sample, as described in the previous section.

ACKNOWLEDGMENTS. We thank Nathan Dalleska and the Environmental Analysis Center for assistance with the metal analyses. The work was supported in part by National Institutes of Health Grant GM045162, by the Howard Hughes Medical Institute, and by fellowships to O.L. from the Fulbright Foundation and the Jane Coffin Childs Memorial Fund for Medical Research.

1. Thompson KH, Orvig C (2003) Boon and bane of metal ions in medicine. *Science* 300:936–939.
2. Helbig K, Grosse C, Nies DH (2008) Cadmium toxicity in glutathione mutants of *Escherichia coli*. *J Bacteriol* 190:5439–5454.
3. Nies DH (2003) Efflux-mediated heavy metal resistance in prokaryotes. *FEMS Microbiol Rev* 27:313–339.
4. Bull PC, Thomas GR, Rommens JM, Forbes JR, Cox DW (1993) The Wilson disease gene is a putative copper transporting P-type ATPase similar to the Menkes gene. *Nat Genet* 5:327–337.
5. Vulpe C, Levinson B, Whitney S, Packman S, Gitschier J (1993) Isolation of a candidate gene for Menkes disease and evidence that it encodes a copper-transporting ATPase. *Nat Genet* 3:7–13.
6. Axelsen KB, Palmgren MG (1998) Evolution of substrate specificities in the P-type ATPase superfamily. *J Mol Evol* 46:84–101.
7. Argüello JM (2003) Identification of ion-selectivity determinants in heavy-metal transport P_{1B}-type ATPases. *J Membr Biol* 195:93–108.
8. Argüello JM, Eren E, González-Guerrero M (2007) The structure and function of heavy metal transport P_{1B}-ATPases. *Biometals* 20:233–248.
9. Fan B, Rosen BP (2002) Biochemical characterization of CopA, the *Escherichia coli* Cu(I)-translocating P-type ATPase. *J Biol Chem* 277:46987–46992.
10. Wu CC, et al. (2006) The cadmium transport sites of CadA, the Cd^{2+}-ATPase from *Listeria monocytogenes*. *J Biol Chem* 281:29533–29541.
11. Gilbert HF (1990) Molecular and cellular aspects of thiol-disulfide exchange. *Adv Enzymol* 63:69–172.
12. Schafer FQ, Buettner GR (2001) Redox environment of the cell as viewed through the redox state of the glutathione disulfide/glutathione couple. *Free Radical Biol Med* 30:1191–1212.
13. Rensing C, Fan B, Sharma R, Mitra B, Rosen BP (2000) CopA: An *Escherichia coli* Cu(I)-translocating P-type ATPase. *Proc Natl Acad Sci USA* 97:652–656.
14. Sharma R, Rensing C, Rosen BP, Mitra B (2000) The ATP hydrolytic activity of purified ZntA, a Pb(II)/Cd(II)/Zn(II)-translocating ATPase from *Escherichia coli*. *J Biol Chem* 275:3873–3878.
15. Lewinson O, Lee AT, Rees DC (2008) The funnel approach to the precrystallization production of membrane proteins. *J Mol Biol* 377:62–73.
16. Grass G, et al. (2001) ZitB (YbgR), a member of the cation diffusion facilitator family, is an additional zinc transporter in *Escherichia coli*. *J Bacteriol* 183:4664–4667.
17. Jacobs MA, et al. (2003) Comprehensive transposon mutant library of *Pseudomonas aeruginosa*. *Proc Natl Acad Sci USA* 100:14339–14344.
18. Neidhardt FC, Umbarger HE (1996) Chemical composition of *Escherichia coli*. *Escherichia coli and Salmonella: Cellular and Molecular Biology*, eds Neidhardt FC, et al. (Am Soc Microbiol, Washington, DC), 2nd Ed, Vol 1, pp 13–16.
19. Finney LA, O'Halloran TV (2003) Transition metal speciation in the cell: insights from the chemistry of metal ion receptors. *Science* 300:931–936.
20. Mitra B, Sharma R (2001) The cysteine-rich amino-terminal domain of ZntA, a Pb(II)/Zn(II)/Cd(II)-translocating ATPase from *Escherichia coli*, is not essential for its function. *Biochemistry* 40:7694–7699.
21. Hatori Y, Majima E, Tsuda T, Toyoshima C (2007) Domain organization and movements in heavy metal ion pumps: Papain digestion of CopA, a Cu^{+}-transporting ATPase. *J Biol Chem* 282:25213–25221.
22. Mana-Capelli S, Mandal AK, Argüello JM (2003) *Archaeoglobus fulgidus* CopB is a thermophilic Cu^{2+}-ATPase: functional role of its histidine-rich-N-terminal metal binding domain. *J Biol Chem* 278:40534–40541.
23. Mandal AK, Yang Y, Kertesz TM, Argüello JM (2004) Identification of the transmembrane metal binding site in Cu^{+}-transporting P_{1B}-type ATPases. *J Biol Chem* 279:54802–54807.
24. Legatzki A, Grass G, Anton A, Rensing C, Nies DH (2003) Interplay of the Czc system and two P-type ATPases in conferring metal resistance to *Ralstonia metallidurans*. *J Bacteriol* 185:4354–4361.
25. Phung LT, Ajlani G, Haselkorn R (1994) P-type ATPase from the cyanobacterium *Synechococcus* 7942 related to the human Menkes and Wilson disease gene products. *Proc Natl Acad Sci USA* 91:9651–9654.
26. Liu J, Dutta SJ, Stemmler AJ, Mitra B (2006) Metal-binding affinity of the transmembrane site in ZntA: implications for metal selectivity. *Biochemistry* 45:763–772.
27. Bal N, Wu CC, Catty P, Guillain F, Mintz E (2003) Cd^{2+} and the N-terminal metal-binding domain protect the putative membranous CPC motif of the Cd^{2+}-ATPase of *Listeria monocytogenes*. *Biochem J* 369:681–685.
28. Dutta SJ, Liu J, Hou Z, Mitra B (2006) Conserved aspartic acid 714 in transmembrane segment 8 of the ZntA subgroup of P1B-type ATPases is a metal-binding residue. *Biochemistry* 45:5923–5931.
29. Trenor C, III, Lin W, Andrews NC (1994) Novel bacterial P-type ATPases with histidine-rich heavy-metal-associated sequences. *Biochem Biophys Res Commun* 205:1644–1650.
30. Johnson TJ, Siek KE, Johnson SJ, Nolan LK (2005) DNA sequence and comparative genomics of pAPEC-O2-R, an avian pathogenic *Escherichia coli* transmissible R plasmid. *Antimicrob Agents Chemother* 49:4681–4688.
31. Francis MS, Thomas CJ (1997) Mutants in the CtpA copper transporting P-type ATPase reduce virulence of *Listeria monocytogenes*. *Microb Pathog* 22:67–78.
32. Papp-Wallace KM, Maguire ME (2006) Manganese transport and the role of manganese in virulence. *Annu Rev Microbiol* 60:187–209.
33. Agranoff DD, Krishna S (1998) Metal ion homeostasis and intracellular parasitism. *Mol Microbiol* 28:403–412.
34. Melchers K, et al. (1998) Properties and function of the P type ion pumps cloned from *Helicobacter pylori*. *Acta Physiol Scand Suppl* 643:123–135.
35. Krogh A, Larsson B, von Heijne G, Sonnhammer EL (2001) Predicting transmembrane protein topology with a hidden Markov model: Application to complete genomes. *J Mol Biol* 305:567–580.